Research Article | Vol. 27, No. 24 / 25 November 2019 / Optics Express 35041
Optics EXPRESS

Ultra low-noise coherent supercontinuum amplification and compression below 100 fs in an all-fiber polarization-maintaining thulium fiber amplifier

ANUPAMAA RAMPUR,[1,2,*] YURIY STEPANENKO,[2] GRZEGORZ STĘPNIEWSKI,[3] TOMASZ KARDAŚ,[4] DOMINIK DOBRAKOWSKI,[1,3] DIRK-MATHYS SPANGENBERG,[5] THOMAS FEURER,[5] ALEXANDER HEIDT,[5] AND MARIUSZ KLIMCZAK[1,3]

[1] University of Warsaw, Faculty of Physics, Pasteura 5, 02-093 Warsaw, Poland
[2] Institute of Physical Chemistry, Polish Academy of Sciences, Kasprzaka 44/52, 01-224 Warsaw, Poland
[3] Institute of Electronic Materials Technology, Glass Department, Wólczyńska 133, 01-919 Warsaw, Poland
[4] FLUENCE Sp. z o. o., Kasprzaka 44/52, 01-224 Warsaw, Poland
[5] Institute of Applied Physics, University of Bern, Sidlerstrasse 5, 3012 Bern, Switzerland
[*] anupamaa.rampur@fuw.edu.pl

Abstract: We report an ultra-low noise, polarization-maintaining, ultrafast Thulium-doped all-fiber chirped pulse amplifier, seeded by a polarized all-normal dispersion (ANDi) supercontinuum (SC) driven by an ultrafast Erbium-fiber laser. The system comprises only polarization-maintaining fibers and delivers 96 fs pulses with 350 mW output power at 100 MHz, centered at 1900 nm. The integrated relative intensity noise (RIN) in the range of 10 Hz – 10 MHz is only 0.047% at the amplifier output, which is virtually identical to the RIN of the Erbium-fiber laser driving the SC. Therefore, neither the SC generation nor the amplification process introduce significant excess noise. The RIN of our system is an order of magnitude lower than similar systems previously seeded with Raman solitons. This highlights the superior noise properties of ANDi SC and their potential as ultra-low noise seed sources for broadband, high power ultrafast fiber amplifiers and frequency combs.

1. Introduction

Broadband coherent seeding of ultrafast rare-earth doped optical amplifiers enables the realization of high peak power, ultrashort pulse light sources using optical fibers. Seeding of an optical parametric chirped pulse amplifier with a femtosecond-pumped, pulse-preserving supercontinuum enabled demonstration of carrier-envelope phase (CEP)-stable, nearly single-cycle pulses at energy levels compatible with attosecond technology [1]. Coherent seeding of Thulium-doped fiber amplifiers with solitonic seed signals pumped by femtosecond Erbium-doped systems have been reported [2–5], which were successfully applied to the generation of ultrashort pulses and frequency combs in the mid-infrared light via nonlinear frequency conversion [6–11]. In combination with a dispersive wave generated at around 1030 nm, this opens a route to optical-fiber based single-cycle pulse generation by simultaneous seeding of Yb^{3+} and Tm^{3+} doped amplifiers, albeit under the rigor of precise control of soliton fission and modulation instability driven decoherence of the seed signal [12].

Many reported ultrafast fiber amplifier systems operating in the 2 µm spectral range are coherently seeded by modelocked Erbium (Er)-fiber systems, which are spectrally broadened to around 2 µm wavelengths through the generation of Raman-shifted solitons, four-wave mixing, or supercontinuum (SC) generation in spectral range, where a highly nonlinear fibers has anomalous

#376203 https://doi.org/10.1364/OE.27.035041
Journal © 2019 Received 17 Sep 2019; revised 5 Nov 2019; accepted 5 Nov 2019; published 15 Nov 2019

Optics EXPRESS

dispersion [2–5,8–10,13]. This allows the straightforward extension of the maturity and excellent performance parameters of Er:fiber technology to longer wavelengths and easy power scaling. The drawback of this solution is that nonlinear dynamics pumped in the anomalous dispersion regime of an optical fiber are very sensitive to the amplification of noise due to modulation instability [14]. The resulting intensity noise and phase fluctuations are then further increased in the subsequent amplifier system. Consequently, the reported relative intensity noise (RIN) values of such systems operating in the 2 μm waveband are in the range 0.2–0.7%, depending on implementation details and noise frequency integration range, which is about an order of magnitude larger than the driving Er:fiber seed [5,8–11,15]. For instance, for a Thulium-Holmium (Tm/Ho) co-doped fiber amplifier seeded by a solitonic SC a RIN value of 0.23% was reported, integrated over the narrow frequency range 1 kHz – 1 MHz, corresponding to an increase of the seed signal noise by a factor of 57 times [11]. Similar RIN values were reported for a Tm/Ho co-doped amplifier seeded with a Raman soliton signal (0.6%, 1 Hz to 10 MHz) [5], a supercontinuum-seeded hybrid Er/Tm fiber frequency comb source (0.7%, 1 Hz to 1 MHz) [9], and a frequency comb system operating in the 2–2.15 μm wavelength range seeded by Raman solitons (0.3%,1 Hz to 10 MHz) [10]. Recently, amplification of white noise during the nonlinear broadening of the Er-fiber seed system in the anomalous dispersion region of a highly nonlinear fiber has been identified as one of the major performance limitations for the further evolution of high power frequency combs at 2 μm, leading to 0.5% of integrated RIN (10 Hz – 30 MHz) at the amplifier output. [8] Direct amplification schemes of Tm-doped mode-locked fiber lasers using anomalous dispersion nonlinear dynamics for pulse shortening, such as nonlinear self-compression, face similar noise challenges (e.g. 0.34% RIN in a frequency range from 10 Hz to 11 MHz in a recently reported 50 fs system) [15].

Compared to its anomalously pumped counterpart, all-normal dispersion (ANDi) supercontinuum exhibits a much superior noise performance [16–18]. This is a result of the fact that many nonlinear noise amplifying effects, such as scalar modulation instability or the Raman effect, are effectively suppressed by the ANDi design and the associated nonlinear dynamics [16]. ANDi engineered photonic crystal fibers (PCFs), compatible with pumping at the wavelength of around 1560 nm, offer the potential for pulse-preserving supercontinuum generation covering amplification bands of all the three major fiber amplifiers [19]. Coherent seeding of a Tm/Ho co-doped fiber amplifier system with this type of supercontinuum was recently demonstrated, resulting in 66 fs pulses, centered at 1940 nm with 100 nm of 3 dB width and 70 kW of peak power [20]. However, this work has also revealed that in a non-PM system architecture, polarization modulational instability (PMI) becomes the major performance-limiting factor in ANDi SC seeded amplifiers, as it occurs both in normal and anomalous dispersion regimes. PMI leads to significant pulse-to-pulse fluctuations and coherence degradation of SC pulses specifically in weakly birefringent fibers, as reported in detail in [21–23]. In the amplitude noise spectrum, the occurrence of PMI is associated with the generation of a significant white-noise component [20,24] However, PMI can be efficiently suppressed in highly birefringent, polarization-maintaining (PM) fibers, eliminating the last remaining noise amplification process in femtosecond pumped ANDi SC generation [24].

In this work, we show that a combination of SC generation in a PM ANDi fiber and its amplification in a fully PM fiber system indeed eliminates all major sources of nonlinear noise amplification and enables ultra-low noise performance of ultrashort pulse amplifiers and frequency comb sources in the 2 μm spectral region. This is evidenced with results of RIN measurements, executed for the driving femtosecond Er:fiber laser front-end, the ANDi SC and the Thulium-doped fiber amplifier, revealing virtually identical integrated RIN figures. Therefore, neither the SC generation nor the amplification process introduce significant excess noise. The integrated RIN of our system is an order of magnitude lower than previous reports employing anomalous dispersion nonlinear dynamics for seeding ultrafast fiber amplifiers at 2 μm.

Optics EXPRESS

2. Experimental setup

The experimental setup for pulse amplification is shown in Fig. 1. We employ the chirped pulse amplification configuration. [25] At the front end, there is a 15 cm long PM ANDi PCF, selected specifically for broadband seeding of ultrafast Tm fiber amplifiers. Although the nonlinear dynamics are effectively concluded within the first few millimeters of the PCF (the optical wavebreaking length is about 4 mm), the length of the PCF was chosen to increase the convenience of handling. The different architectures and characteristics of highly nonlinear PM PCF designs were investigated in earlier work [26], including detailed measurement description of dispersion and group birefringence. Figure 2 shows the measured dispersion and birefringence characteristics of the chosen design, along with an inset image of the PM ANDi PCF structure from a scanning electron microscope. Here, birefringence was induced by the deformed photonic lattice with an elliptical core. The dispersion profile is flat and all-normal within ± 10 ps/nm/km around -60 ps/nm/km at the intended pump wavelength of 1560 nm, and the birefringence is in the order of 10^{-4}. The difference of chromatic dispersion between X and Y axis is around 3 to 5 ps/nm/km in the range between 1500 nm and 2000 nm. The PM ANDi PCF is pumped by a commercial Er:fiber-based laser (Menlo Systems) operating at a central wavelength of 1560 nm with 100 MHz repetition rate, delivering 80 fs long, 3.5 nJ Gaussian pulses. The pulse energy coupled into the PM PCF is estimated to 2 nJ. Although the PCF supports multiple higher-order modes up to around 1700 nm (as confirmed by linear simulations), selective single fundamental mode excitation is possible and was validated experimentally by imaging the PCF output by using a camera with a 1560 nm sensitive phosphor layer.

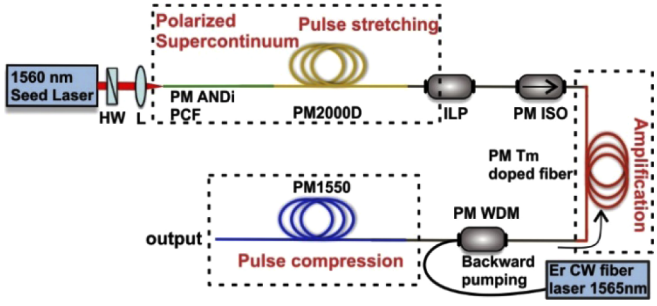

Fig. 1. Experimental setup of coherently seeded ultrafast all-PM thulium fiber amplifier. HW – half-wave plate, L - aspheric lens, PM ANDi PCF - polarization maintaining all normal dispersion photonic crystal fiber, ILP - inline polarizer, PM ISO - polarization maintaining isolator, PM WDM - polarization maintaining wavelength division multiplexer, Er CW – Erbium-doped continuous wave fiber laser.

A half-wave plate at the input and a polarizer at the output of the PCF were used to differentiate between the polarization components of the fundamental mode at the output of the PCF in order to match the polarization to that of the active fiber of the amplifier. The PM PCF generates spectrally broad (1100-2150 nm) and coherent supercontinuum with 40 mW of output power. We did not identify which of the axes was fast or slow but observed a small difference of broadening of 20 nm at the long-wavelength edge of the supercontinuum spectrum. The difference is due to the slightly different dispersion along the axes of PCF, as shown in Fig. 2. Hence, we fixed the position of the half-wave plate to the axis with the broadest available spectrum. The supercontinuum is linearly polarized with around 10 dB of polarization extinction ratio. Figure 3 shows the SC spectrogram recorded using cross-correlation frequency-resolved optical gating (XFROG). It is evident that SC in PM ANDi PCF is dominated by self-phase modulation and optical wave breaking, the normal dispersion nonlinear processes, which preserve the temporal

Optics EXPRESS

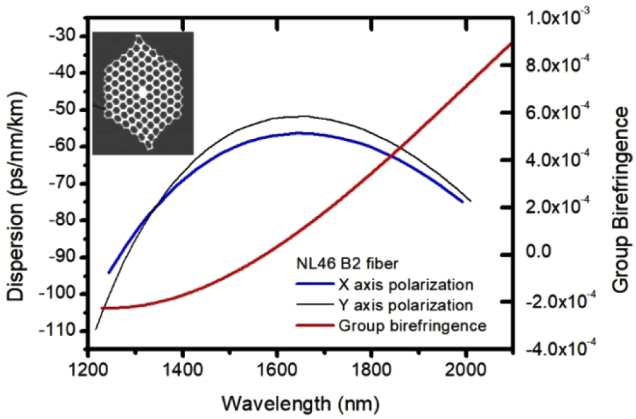

Fig. 2. Measured group birefringence and chromatic dispersion along both axes of the PM ANDi PCF. The inset shows a scanning electron microscopy image of the fiber structure.

integrity of the pump pulse. The spectrogram shows that the SC pulse is positively chirped along the entire pulse length. The spectral marginal in Fig. 3 shows good correspondence over the entire spectral width between the supercontinuum spectrum measured with an optical spectrum analyzer (OSA) and the spectrum retrieved from the XFROG measurement. We obtain 8 ps long pulses after the PCF as shown in the temporal marginal.

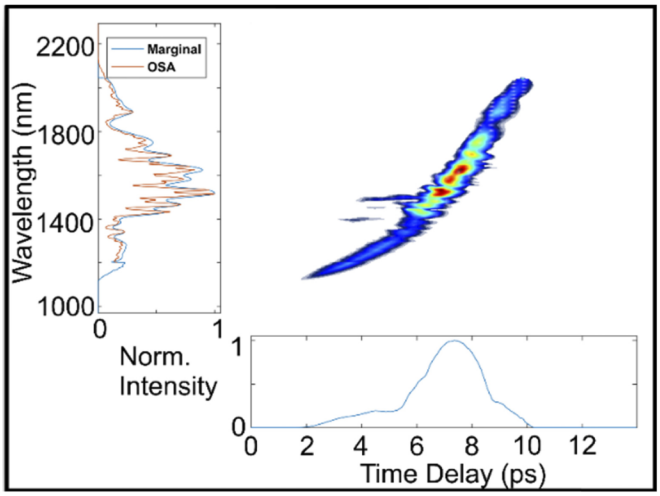

Fig. 3. Measured group delay trace of the coherent ANDi supercontinuum seed signal using cross-correlation frequency-resolved optical gating. Left: Comparison of supercontinuum spectra retrieved from XFROG and measured with OSA (linear scale). Bottom: retrieved pulse shape.

In the following experiment, the polarizer at the output of the PM ANDi PCF was removed and butt-coupled to 9 m long, polarization maintaining PM2000D fiber (Coherent Nufern) in order to further temporally stretch the seed pulse before amplification. Due to the mismatch of core diameters and thermal expansion coefficients between the two fibers, standard fusion splicing was not possible. Thus, we placed the PM2000D fiber on a rotation mount to match its polarization axis with PM ANDi PCF axis. All the remaining fibers in the setup were fusion spliced with a standard PM fiber compatible splicer (Ericsson FSU-995). We note that cold splicing of the

Optics EXPRESS

silicate glass ANDi PCF used here to a silica single-mode fiber is generally possible by moving the splicing arc away from the PCF to heat up the silica fiber only. This, however, limits the seed signal average power due to a lossy splice and was not implemented in this work. The PM2000D fiber has positive flattened group velocity dispersion (GVD) of around 0.05 to 0.1 ps^2/m in the range of 1420–2200 nm, as shown in Fig. 4, which is well suited for chirp management in fiber-based ultrafast systems operating around 1900-2000 nm [27].

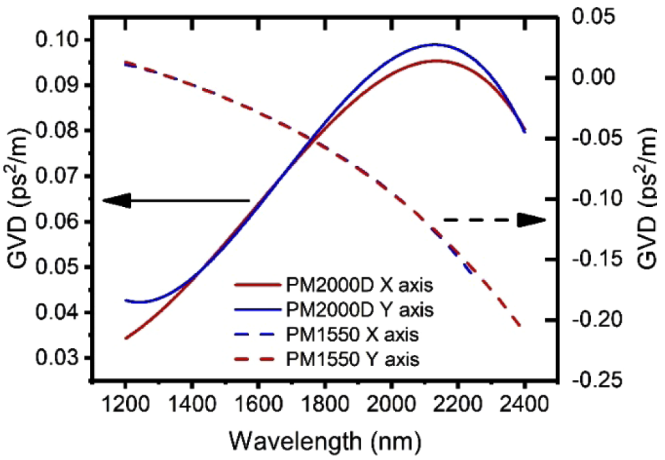

Fig. 4. Measured group velocity dispersion characteristics of the PM2000D and PM1550 fiber (representing Tm-doped fiber), adapted from [27];

An in-line fiber polarizer (ILP) was used to remove any remaining depolarized components before the seed was forwarded to the Tm-doped fiber. The amplification stage consisted of a 5 m long section of PM single-mode thulium-doped fiber (Coherent Nufern PM-TSF-9/125), backward core pumped by a continuous-wave (CW) signal. The pump signal was delivered through a PM wavelength division multiplexer (PM WDM) by an in-house built CW erbium-ytterbium (Er + Yb) fiber amplifier operating typically at 1 W of output power at 1565 nm. Group velocity dispersion (GVD) of the standard single-mode PM1550 fiber and PM2000D fiber is shown in Fig. 4. Tm-doped PM-TSF-9/125 fiber's GVD is assumed as that of PM1550 fiber, having a negative slope of around -0.15 to -0.01 ps^2/m in the range 1420–2000 nm.

A polarization maintaining isolator (PM ISO) was used to ensure unidirectional operation of the amplifier. Since these commercial fiber components were available in the "fast axis blocked" variant as standard, the developed system operates in the slow axis. The PM architecture of the setup did not require any polarization controllers. Pulse compression was achieved by splicing an appropriate length of PM1550 fiber to the amplifer. The amplifier output and pulse compression were monitored with an OSA and an in-house built, second harmonic generation, frequency-resolved optical gating (SHG-FROG) setup, respectively. Additionally, we measured the relative intensity noise of PM Tm amplifier and the supercontinuum seed pump laser using a 12.5 GHz, 2 μm InGaAs photodiode and an RF spectrum analyzer (Agilent E4443A) employing the standard procedures outlined in literature. [28]

3. Results and discussions

We begin by measuring the spectrum of the amplified pulses at the output of the amplifier. Fig. 5 shows the long wavelength part of the supercontinuum seed signal (black) and the amplified spectrum at the output of Tm fiber amplifier (dark blue). The spectrum of the pulses at the output of the amplifier is shaped mostly by the Tm-doped fiber gain profile, but also by the filtering

Optics EXPRESS

effect of the PM WDM. At the amplifier output, we obtained 350 mW of average output power with 84 nm of 3 dB spectral width, centered at 1900 nm, and 16 dB polarization extinction. In the following steps, we purposefully did not drive the amplifier to high output powers and focused on the feasibility of all-fiber compensation of the output pulse chirp and on the noise performance of the system. It is important to note that the octave spanning supercontinuum seed is first stretched to 286 ps along the 9 m long, positive GVD PM2000D fiber to avoid nonlinearities and switch of chirp sign during amplification. Further, the seed signal is simultaneously amplified and slightly compressed along propagation in the negative GVD Tm-doped fiber. The length of normal and anomalous dispersion dispersion active and passive fibers were adjusted such that the amplified pulse at the end of the amplifier is still positively chirped.

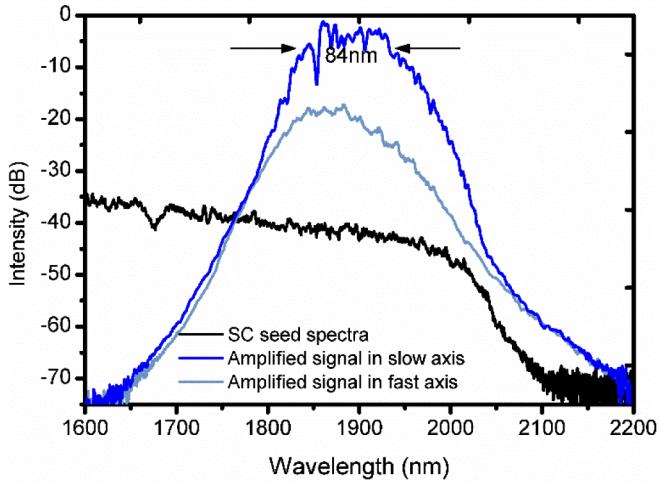

Fig. 5. Logarithmic scale spectra of the amplifier seed pulse (black) and the amplified signal in slow axis (dark blue) and in fast axis (light blue). The all-fiber PM Tm fiber amplifier system operates in slow axis.

Figure 6 shows the SHG-FROG traces retrieved using an algorithm based on generalized projections [29]. At the output of the amplifier prior to recompression, the retrieved pulse duration was 3.6 ps as shown in Fig. 6(a). Figure 6(b) shows the FROG trace measured at the end of 2 m of PM1550 fiber spliced to the output of the amplifier for pulse compression. We obtained 1.7 ps retrieved pulse duration with a flip in symmetry, indicating that dispersion was over-compensated due to excessive length of the compensating fiber at the amplifier output. FROG traces in Fig. 6(a) and Fig. 6(b) show the characteristic flip in the symmetry, which helps to distinguish the cross over point during compression. From this point, we used the cut-back method to compensate for the GVD and monitored the output group delay profile for each cut length to attain compression.

Figures 7(a) and 7(b) show the measured and retrieved FROG traces for the optimal length of the PM1550 fiber used to recompress the output pulse. Wavelength scale is converted back to the original from the SHG wavelength. The FROG retrieval error was 5.4×10^{-3} over a 512×512 grid size. A small mismatch between the FROG-reconstructed spectrum and experimental spectrum measured with OSA as shown in Fig. 7(c) is assigned to spectrometer calibration. The fine structure observed in the spectrum of the compressed pulse at the system output is likely due to a birefringent filtering effect, caused by a slight misalignment of the fiber polarization axes before a polarization sensitive element. We verified that the amplifier output signal is not polarization sensitive, by disturbing the fibers during operation of the amplifier. The color map of the FROG trace revealed that more than 60% of the total energy was concentrated in the main

Optics EXPRESS

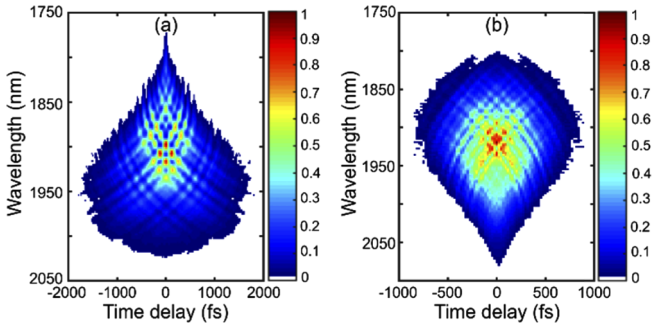

Fig. 6. Retrieved output pulse spectrograms (a) at the output of the Tm fiber prior to recompression (b) after 2 m of additional PM1550 fiber.

part of the pulse. The pulse duration was 96 fs (blue curve) considering the Gaussian pulse shape, as shown in Fig. 7(d). The calculated transform-limited pulse length is 69 fs (black curve). The compressed pulse has a time-bandwidth product (TBP) of 0.697, which is 1.6 times larger than the transform-limited pulse. This is due to the accumulation of significant third-order dispersion (TOD) over the length of the all-fiber system, as the simultaneous compensation of GVD and TOD using only optical fibers is not possible. Further power scaling is feasible, however, the current limitation is the pump power. Moreover, the small mode field diameter of the PM1550 fiber used as compressor distorts the pulse at high pulse energies due to nonlinear effects. Large mode area (LMA) fibers or external compression using bulk optics, such as gratings or chirped

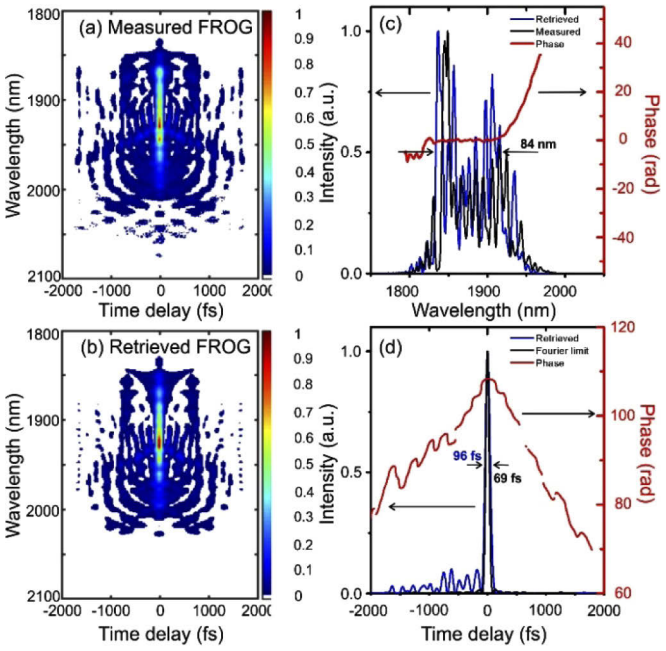

Fig. 7. Characterization of the compressed pulse at the output of the PM1550 fiber using SHG FROG. (a) Measured FROG trace, (b) Retrieved FROG trace, (c) FROG-retrieved spectrum (blue) compared to spectrum independently measured with an OSA (black) and phase profile (red), (d) FROG-retrieved pulse shape (blue) compared to the Fourier limit (black) and phase profile (red).

Optics EXPRESS

mirror pairs, could be used for pulse compression even at high pulse energies. Higher-order dispersion and nonlinear effects in the compression stage will be examined in a further study, along with power scaling.

The amplified pulse at the end of the Tm-doped fiber is recompressed to 96 ± 0.5 fs with an average output power of 350 mW and pulse energy of 3.5 nJ.

In the final stage of the work, we performed a noise characterization of the developed amplification system. RIN measurements were performed using a 12.5 GHz InGaAs broadband photodiode (PD) sensitive over the entire spectral bandwidth of the SC. (ET-5000F from Electro-Optics Technology). Agilent E4443A electronic spectrum analyzer (ESA) was used to record the Radio Frequency (RF) spectrum. The light from the amplifier system was directly coupled into the PD using a single-mode fiber. For the linear operation of the PD, the power was maintained around 1 mW and the DC photocurrent was monitored at the output of the photodiode using a digital multimeter. The DC power is obtained as $P_{DC} = (I_{DC})^2 \cdot R_L$, where I_{DC} stands for the DC current and R_L is the load resistance of the ESA. Figure 8 shows the measured intensity noise of the Er:fiber seed laser, the supercontinuum, and the Tm-doped fiber amplifier. The relative intensity shot noise level of the PD was calculated for the seed laser and Tm amplifier as P_{shot}/P_{DC}, where P_{shot} is shot noise power $2qI_{DC}R_L$, and q is the elementary charge. Therefore, the RIN (shot) is determined by $2q/I_{DC}$. In our measurements, the shot noise limit was equal to −154.13 dB/Hz, −153.85 dB/Hz and −154.08 dB/Hz for Tm amplifier, ANDi supercontinuum, and the Er:fiber seed laser, respectively. The RIN (shot) levels are slightly different due to different I_{DC} values for the amplifier, supercontinuum and the seed laser.

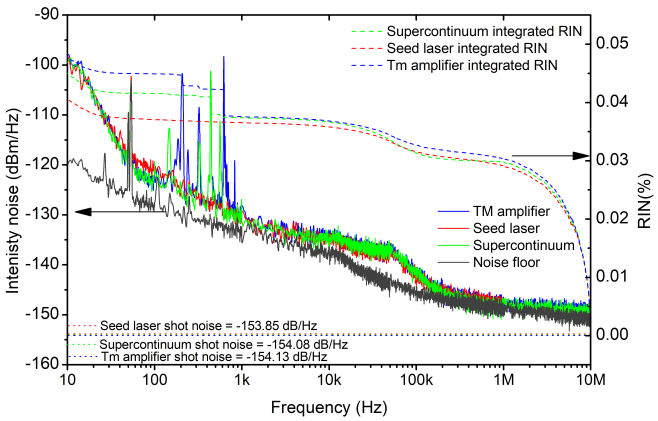

Fig. 8. Measured noise characteristics of the Tm amplifier (solid blue), Er:fiber seed laser (solid red) and ANDi supercontinuum (solid green). The dotted lines indicate the shot-noise limit corresponding to the Tm amplifier (blue dot), seed laser (red dot) and supercontinuum (green dot). The black continuous line is the noise floor of the photodiode. The right y-axis shows the integrated RIN of the Tm amplifier (blue dash), the Er:fiber seed laser (red dash) and the ANDi supercontinuum (green dash).

The results of our RIN measurements are shown in Fig. 8. The sensitivity limit given by the noise floor of the photodiode is indicated by the black continuous. Remarkably, the RIN of both the ANDi SC and the amplifier are virtually identical to the RIN of the Er:fiber seed laser, apart from some additional low-frequency noise peaks < 1 kHz attributed to mechanical vibrations at the free-space PCF coupling port and pump diode noise from the CW amplifier used to pump the Tm-doped fiber amplifier. Hence, neither the nonlinear spectral broadening nor the subsequent amplification process introduce significant excess noise. Most importantly, we do not observe any

Optics EXPRESS

signatures of noise-amplifying nonlinear effects such as scalar or polarization MI, which have been linked in previous reports to the occurrence of white-noise high-frequency components in the amplitude noise spectrum [8,14,20,24]

The integrated RIN is calculated from 10 Hz to 10 MHz and represented on the right y-axis in Fig. 8. For the Er:fiber seed laser, the RIN is determined as 0.040%, while for the ANDi supercontinuum it is 0.045% and for the Tm-doped fiber amplifer 0.047%. This corresponds to less than 20% excess noise introduced by the nonlinear broadening stage and the power amplifier combined. Hence, the integrated RIN at the output of the amplifier developed in this work is in the order of one magnitude lower than the previous results using anomalous dispersion nonlinear dynamics for spectral broadening of the Er:fiber seed laser.

4. Conclusion

The successful amplification and recompression of all-normal dispersion supercontinuum pulses provide experimental evidence for the feasibility of ultra-low noise, coherent seeding of ultrafast fiber amplifiers operating at pulse duration below 100 fs in the 2 μm wavelength window. While we did not reach the Fourier transform limit in the current implementation due to the unavailability of fibers allowing simultaneous higher-order dispersion compensation, this could still be worked around at a power amplifier stage with an external compressor. Compared to earlier realizations of ultrafast seeding of fiber amplifiers using anomalous dispersion nonlinear dynamics, the major advance of our system is the elimination of noise amplifying nonlinear effects from the spectral broadening and amplification stages. Normal dispersion nonlinear dynamics have recently been reported to have a factor of 50 higher intensity threshold for modulation instability-driven decoherence compared to anomalous dispersion dynamics [16]. The polarization maintaining design of both the nonlinear fiber and amplifier makes our system also immune against PMI instabilities, which have recently been identified as major performance limitation in non-polarization-maintaining systems, even when seeded by ANDi SC sources [20]. The exclusion of all decoherence-driving nonlinear effects finds reflection in our RIN measurement results, which revealed a factor of 10 improvement over systems using anomalous dispersion nonlinear dynamics for seed signal generation. Noise amplification in our system is limited to only 20%, mainly caused by low-frequency noise originating from the pump diodes. Conveniently, our results add up with the improved threshold for transverse mode-instability in Tm-doped ultrafast fiber amplifiers, as compared to Yb-doped systems [30]. The developed system follows an all-polarization maintaining design, including the nonlinear fiber for the generation of coherent supercontinuum for the seed signal. Low noise inherent to this type of supercontinuum, combined with a determined state of polarization across the entire setup, contributed to excellent noise properties of the amplifier, which practically replicated those of the seed femtosecond laser at the front-end of the system. The amplifier's robustness and environmental stability stemming from the all-PM fiber configuration make it a promising platform for further power scaling and, for example, pulse synthesis using a tandem of simultaneously seeded Er-doped and Tm-doped fiber amplifiers.

Funding

Fundacja na rzecz Nauki Polskiej (FNP) (First TEAM/2016-1/1 - POIR.04.04.00-00-1D64/16-00); Schweizerischer Nationalfonds zur Förderung der Wissenschaftlichen Forschung (SNSF) (PCEFP2_181222); Narodowe Centrum Nauki OPUS (2017/25/B/ST7/01145); Schlumberger Foundation Faculty for the Future program (Anupamaa Rampur).

Acknowledgments

Chenchen Wan from Thorlabs is acknowledged for fruitful discussions on RIN measurements.

Optics EXPRESS

Disclosures

YS: Fluence Sp. z o. o. (E), TK: Fluence Sp. z o. o. (E). The remaining authors declare no conflicts of interest.

References

1. J. Rothhardt, S. Demmler, S. Hädrich, J. Limpert, and A. Tünnermann, "Octave-spanning OPCPA system delivering CEP-stable few-cycle pulses and 22 W of average power at 1 MHz repetition rate," Opt. Express **20**(10), 10870–10878 (2012).
2. S. Kumkar, G. Krauss, M. Wunram, D. Fehrenbacher, U. Demirbas, D. Brida, and A. Leitenstorfer, "Femtosecond coherent seeding of a broadband Tm:fiber amplifier by an Er:fiber system," Opt. Lett. **37**(4), 554–556 (2012).
3. G. Soboń, T. Martynkien, K. Tarnowski, P. Mergo, and J. Sotor, "Generation of sub-100 fs pulses tunable from 1700 to 2100 nm from a compact frequency-shifted Er-fiber laser," Photonics Res. **5**(3), 151–155 (2017).
4. G. Soboń, T. Martynkien, D. Tomaszewska, K. Tarnowski, P. Mergo, and J. Sotor, "All-in-fiber amplification and compression of coherent frequency-shifted solitons tunable in the 1800–2000 nm range," Photonics Res. **6**(5), 368–372 (2018).
5. N. Coluccelli, M. Cassinerio, P. Laporta, and G. Galzerano, "Single-clad Tm–Ho:fiber amplifier for high-power sub-100-fs pulses around 1.9 μm," Opt. Lett. **38**(15), 2757–2759 (2013).
6. J. Sotor, T. Martynkien, P. G. Schunemann, P. Mergo, L. Rutkowski, and G. Soboń, "All-fiber mid-infrared source tunable from 6 to 9 μm based on difference frequency generation in OP-GaP crystal," Opt. Express **26**(9), 11756–11763 (2018).
7. D. Churin, K. Kieu, R. A. Norwood, and N. Peyghambarian, "Efficient Frequency Comb Generation in the 9 μm Region Using Compact Fiber Sources," IEEE Photonics Technol. Lett. **26**(22), 2271–2274 (2014).
8. C. Gaida, T. Heuermann, M. Gebhardt, E. Shestaev, T. P. Butler, D. Gerz, N. Lilienfein, P. Sulzer, M. Fischer, R. Holzwarth, A. Leitenstorfer, I. Pupeza, and J. Limpert, "High-power frequency comb at 2 μm wavelength emitted by a Tm-doped fiber laser system," Opt. Lett. **43**(21), 5178–5181 (2018).
9. F. Adler and S. A. Diddams, "High-power, hybrid Er:fiber/Tm:fiber frequency comb source in the 2 μm wavelength region," Opt. Lett. **37**(9), 1400–1402 (2012).
10. N. Coluccelli, M. Cassinerio, A. Gambetta, P. Laporta, and G. Galzerano, "High-power frequency comb in the range of 2–2.15 μm based on a holmium fiber amplifier seeded by wavelength-shifted Raman solitons from an erbium-fiber laser," Opt. Lett. **39**(6), 1661–1664 (2014).
11. H. Hoogland, A. Thai, D. Sánchez, S. L. Cousin, M. Hemmer, M. Engelbrecht, J. Biegert, and R. Holzwarth, "All-PM coherent 2.05 μm Thulium/Holmium fiber frequency comb source at 100 MHz with up to 0.5 W average power and pulse duration down to 135 fs," Opt. Express **21**(25), 31390–31394 (2013).
12. G. Krauss, S. Lohss, T. Hanke, A. Sell, S. Eggert, R. Huber, and A. Leitenstorfer, "Synthesis of a single cycle of light with compact erbium-doped fibre technology," Nat. Photonics **4**(1), 33–36 (2010).
13. F. Tan, H. Shi, R. Sun, P. Wang, and P. Wang, "1 μJ, sub-300 fs pulse generation from a compact thulium-doped chirped pulse amplifier seeded by Raman shifted erbium-doped fiber laser," Opt. Express **24**(20), 22461–22468 (2016).
14. N. R. Newbury, B. R. Washburn, K. L. Corwin, and R. S. Windeler, "Noise amplification during supercontinuum generation in microstructure fiber," Opt. Lett. **28**(11), 944–946 (2003).
15. T. Heuermann, C. Gaida, M. Gebhardt, and J. Limpert, "Thulium-doped nonlinear fiber amplifier delivering 50 fs pulses at 20 W of average power," Opt. Lett. **43**(18), 4441–4444 (2018).
16. A. M. Heidt, J. S. Feehan, J. H. V. Price, and T. Feurer, "Limits of coherent supercontinuum generation in normal dispersion fibers," J. Opt. Soc. Am. B **34**(4), 764–775 (2017).
17. D. S. Shreesha Rao, R. D. Engelsholm, I. B. Gonzalo, B. Zhou, P. Bowen, P. M. Moselund, O. Bang, and M. Bache, "Ultra-low-noise supercontinuum generation with a flat near-zero normal dispersion fiber," Opt. Lett. **44**(9), 2216–2219 (2019).
18. E. Genier, P. Bowen, T. Sylvestre, J. M. Dudley, P. Moselund, and O. Bang, "Amplitude noise and coherence degradation of femtosecond supercontinuum generation in all-normal-dispersion fibers," J. Opt. Soc. Am. B **36**(2), A161–A167 (2019).
19. M. Klimczak, B. Siwicki, P. Skibiński, D. Pysz, R. Stępień, A. Heidt, C. Radzewicz, and R. Buczyński, "Coherent supercontinuum generation up to 2.3 μm in all-solid soft-glass photonic crystal fibers with flat all-normal dispersion," Opt. Express **22**(15), 18824–18832 (2014).
20. A. M. Heidt, J. Modupeh Hodasi, A. Rampur, D.-M. Spangenberg, M. Ryser, M. Klimczak, and T. Feurer, "Low noise all-fiber amplification of a coherent supercontinuum at 2 μm and its limits imposed by polarization noise," arXiv e-prints arXiv:1903.09583 (2019).
21. G. Millot, E. Seve, S. Wabnitz, and M. Haelterman, "Observation of induced modulational polarization instabilities and pulse-train generation in the normal-dispersion regime of a birefringent optical fiber," J. Opt. Soc. Am. B **15**(4), 1266–1277 (1998).
22. H. Tu, Y. Liu, X. Liu, D. Turchinovich, J. Lægsgaard, and S. A. Boppart, "Nonlinear polarization dynamics in a weakly birefringent all-normal dispersion photonic crystal fiber: toward a practical coherent fiber supercontinuum laser," Opt. Express **20**(2), 1113–1128 (2012).

Optics EXPRESS

23. I. Bravo Gonzalo, R. D. Engelsholm, M. P. Sørensen, and O. Bang, "Polarization noise places severe constraints on coherence of all-normal dispersion femtosecond supercontinuum generation," Sci. Rep. **8**(1), 6579 (2018).
24. Y. Liu, Y. Zhao, J. Lyngsø, S. You, W. L. Wilson, H. Tu, and S. A. Boppart, "Suppressing Short-Term Polarization Noise and Related Spectral Decoherence in All-Normal Dispersion Fiber Supercontinuum Generation," J. Lightwave Technol. **33**(9), 1814–1820 (2015).
25. D. Strickland and G. Mourou, "Compression of amplified chirped optical pulses," Opt. Commun. **56**(3), 219–221 (1985).
26. D. Dobrakowski, A. Rampur, G. Stępniewski, A. Anuszkiewicz, J. Lisowska, D. Pysz, R. Kasztelanic, and M. Klimczak, "Development of highly nonlinear polarization-maintaining fibers with normal dispersion across entire transmission window," J. Opt. **21**(1), 015504 (2019).
27. P. Ciąćka, A. Rampur, A. Heidt, T. Feurer, and M. Klimczak, "Dispersion measurement of ultra-high numerical aperture fibers covering thulium, holmium, and erbium emission wavelengths," J. Opt. Soc. Am. B **35**(6), 1301–1307 (2018).
28. R. P. Scott, C. Langrock, and B. H. Kolner, "High-dynamic-range laser amplitude and phase noise measurement techniques," IEEE J. Sel. Top. Quantum Electron. **7**(4), 641–655 (2001).
29. K. W. DeLong, D. N. Fittinghoff, R. Trebino, B. Kohler, and K. Wilson, "Pulse retrieval in frequency-resolved optical gating based on the method of generalized projections," Opt. Lett. **19**(24), 2152–2154 (1994).
30. C. Gaida, M. Gebhardt, T. Heuermann, F. Stutzki, C. Jauregui, and J. Limpert, "Ultrafast thulium fiber laser system emitting more than 1 kW of average power," Opt. Lett. **43**(23), 5853–5856 (2018).